

### Reinforced alginate/gelatin sponges functionalized by avidin/biotin binding strategy: a novel cardiac patch

Journal:	<i>Journal of Biomaterials Applications</i>
Manuscript ID	JBA-18-0402.R2
Manuscript Type:	Original Manuscript
Keywords:	polydioxanone, insulin-like growth factor 1, cardiac tissue engineering, suture retention, cardiac patch
Abstract:	<p>Adequate mechanical properties to withstand the surgical procedure and decoration with bioactive molecules promoting tissue regeneration are crucial aspects in the development of successful matrices for cardiac tissue engineering. The aim of this work was the development of a novel cardiac patch based on a blend of alginate and gelatin, designed to combine the improvement of suture resistance with an effective growth factor immobilization. We defined the procedures to incorporate a poly(dioxanone) membrane within the alginate/gelatin sponges and to functionalize the biomaterial with insulin-like growth factor-1, using the avidin-biotin binding strategy. Morphological analysis of the reinforced scaffolds showed a porous structure and a good adhesion of the synthetic microporous membrane to the natural sponge. Infrared chemical imaging analysis demonstrated the efficacy of the chemical treatments performed for scaffold reinforcement and functionalization. A good hydrophilicity and an adequate permeability were shown by swelling and permeability tests. The inclusion of the synthetic membrane improved the viscoelastic properties, as measured by dynamic mechanical analysis, and suture retention force, under both dry and wet conditions. The in vitro and in vivo biological characterization showed that IGF-1 functionalization successfully enhanced cell adhesion and long term retention after implantation on the damaged myocardium, together with improved suturability by PDO reinforcement.</p>

SCHOLARONE™  
Manuscripts

1  
2  
3 Full Title: **Reinforced alginate/gelatin sponges functionalized by avidin/biotin binding**  
4  
5 **strategy: a novel cardiac patch**  
6

7 Short Title: **A novel cardiac patch functionalized with biotinylated growth factor**  
8  
9

10  
11  
12  
13  
14  
15  
16  
17  
18  
19  
20  
21  
22  
23  
24  
25  
26  
27  
28  
29  
30  
31  
32  
33  
34  
35  
36  
37  
38  
39  
40  
41  
42  
43  
44  
45  
46  
47  
48  
49  
50  
51  
52  
53  
54  
55  
56  
57  
58  
59  
60

For Peer Review

## Abstract

Adequate mechanical properties to withstand the surgical procedure and decoration with bioactive molecules promoting tissue regeneration are crucial aspects in the development of successful matrices for cardiac tissue engineering. The aim of this work was the development of a novel cardiac patch based on a blend of alginate and gelatin, designed to combine the improvement of suture resistance with an effective growth factor immobilization. We defined the procedures to incorporate a poly(dioxanone) membrane within the alginate/gelatin sponges and to functionalize the biomaterial with insulin-like growth factor-1, using the avidin-biotin binding strategy. Morphological analysis of the reinforced scaffolds showed a porous structure and a good adhesion of the synthetic microporous membrane to the natural sponge. Infrared chemical imaging analysis demonstrated the efficacy of the chemical treatments performed for scaffold reinforcement and functionalization. A good hydrophilicity and an adequate permeability were shown by swelling and permeability tests. The inclusion of the synthetic membrane improved the viscoelastic properties, as measured by dynamic mechanical analysis, and suture retention force, under both dry and wet conditions. The *in vitro* and *in vivo* biological characterization showed that IGF-1 functionalization successfully enhanced cell adhesion and long term retention after implantation on the damaged myocardium, together with improved suturability by PDO reinforcement.

**Keywords:** polydioxanone, insulin-like growth factor 1, cardiac tissue engineering, suture retention

## 1. Introduction

Cardiovascular diseases represent the first cause of death and disability worldwide [1]. Cardiac cells are not able to efficiently replace the lost myocardium after infarction, ultimately leading to chronic cardiac dysfunction. End-stage heart failure can be currently treated by cardiac transplantation, but this procedure is limited by the shortage of organ donors [2]. Therefore, an increasing demand to develop new therapeutic strategies for patients affected by ischemic cardiomyopathy is still required.

Over the past years, tissue engineering has emerged as a very promising strategy to treat the infarcted myocardium [3]. One of the most important requirements for the development of a successful tissue engineering solution is to mimic the natural tissue microenvironment by polymeric scaffolds able to provide a three-dimensional support promoting myocardial regeneration [4].

Among the different polymeric materials proposed for three-dimensional scaffold fabrication, polymers of natural origin are a promising choice, as they closely resemble the native environment of cardiac cells and are easily susceptible to *in vivo* degradation [5]. Collagen, gelatin, alginate and fibrin have been widely investigated as scaffold materials for myocardial repair. Although scaffolds based on natural polymers represent a promising option, if not appropriately reinforced they lack adequate mechanical strength to withstand the surgical procedures.

In addition to the appropriate selection of materials, another important aspect to achieve a successful cardiac tissue healing by tissue engineering is the “decoration” of the scaffolds with growth factors, which play an important role in promoting cell proliferation and differentiation [6]. However, an effective immobilization of growth factors is still a challenge, because chemical reagents and solvents used for conjugation can alter the biological properties of molecules, such as growth factors, that are easily susceptible to inactivation or denaturation. Moreover, loading methods are usually very expensive, as they require the use of large amount of growth factor to obtain only a partial immobilization.

The aim of this work was the development of a novel cardiac patch, able to improve suture resistance together with an effective growth factor immobilization.

1  
2  
3 The material used for scaffold preparation is a blend of alginate and gelatin, chosen to mimic the  
4 chemical composition and the interactions among components of the cardiac extracellular matrix  
5 (ECM) [7]. Adequate morphological, physicochemical, functional and biological properties of cross-  
6  
7  
8  
9  
10 linked alginate/gelatin sponges have been previously ascertained [8]. However, preliminary  
11  
12  
13  
14  
15  
16 suturability tests, carried out on the alginate/gelatin scaffolds following a procedure described in  
17 literature [9], pointed out an inadequate resistance to sutures (unpublished data).

17 Therefore, in this work a poly(dioxanone) (PDO) membrane was introduced, as reinforcement, in the  
18  
19  
20  
21  
22  
23  
24  
25  
26  
27 core of the alginate/gelatin sponges. PDO was chosen because provided with good flexibility,  
28  
29  
30  
31  
32  
33  
34  
35  
36  
37  
38  
39  
40  
41  
42  
43  
44  
45  
46  
47  
48  
49  
50  
51  
52  
53  
54  
55  
56  
57  
58  
59  
60 elasticity and biocompatibility and is commonly used as suture material [10]. The PDO membrane  
was prepared by phase inversion and the procedure for its inclusion in the core of the alginate/gelatin  
sponge was optimized.

The reinforced sponge was also subjected to functionalization by the avidin-biotin binding system.  
Avidin is a tetrameric glycoprotein found in egg white, with a specific and strong interaction  
(dissociation constant:  $10^{15} \text{ M}^{-1}$ ) with biotin molecules [11]. The avidin-biotin bond is used to  
immobilize biomolecules on different surfaces, for several applications including chromatography,  
diagnostics, immunoassay, drug delivery [12]. Applications in the field of cell culture [13] and tissue  
engineering [14, 15] have been also investigated. However, to the best of our knowledge, the avidin-  
biotin binding strategy to produce functionalized three-dimensional preformed scaffolds for cardiac  
tissue engineering was never tested. Here the idea was to use, in the preparation of the scaffolds, a  
biotinylated gelatin, so that biotin is exposed on scaffold surface; avidin is then used as a bridge  
between biotin on scaffold surface and a biotinylated growth factor. Insulin-like growth factor-1  
(IGF-1) was chosen for functionalization because of its ability to promote survival, homing,  
engraftment and differentiation of cardiac progenitor cells, as well as to improve revascularization  
[16-18].

The overall device concept is drafted in figure 1.

1  
2  
3 Developed prototypes underwent a complete characterization, including morphological,  
4 physicochemical, mechanical and functional analysis. *In vitro* cell culture tests were performed in  
5 order to evaluate the response of cardiac progenitor cells. Furthermore, *in vivo* tests were carried out  
6 in a small animal model.  
7  
8  
9  
10  
11  
12

## 13 14 **2. Materials and methods**

### 15 16 *2.1 Materials*

17  
18 Alginic acid sodium salt (viscosity of 2% solution at 25°C ca. 250 cps), gelatin (type B from bovine  
19 skin), PDO, 1-(3-dimethylaminopropyl)-3-ethylcarbodiimide hydrochloride (EDC), N-  
20 hydroxysuccinimide (NHS), avidin, glutaraldehyde (GTA, 25% aqueous solution) and phosphate  
21 buffered saline (PBS) were supplied by SIGMA (St. Louis, MO). Biotinylated gelatin and  
22 biotinylated IGF-1 were provided by ibt-immunological and biochemical test systems GmbH  
23 (Binzwangen, DE). Hydrochloride solution, sodium hydroxide pellets, calcium chloride and dimethyl  
24 sulfoxide (DMSO) were from Carlo Erba Reagenti (Italy). All the other reagents were commercially  
25 available and used as received.  
26  
27  
28  
29  
30  
31  
32  
33  
34  
35  
36  
37  
38  
39

### 40 *2.2 Preparation of PDO reinforced alginate/gelatin scaffold*

41  
42 A 10% w/v PDO solution in DMSO was prepared under constant stirring at 70°C. The solution was  
43 casted uniformly on a Teflon plate using a knife machine with a velocity of 1 m/min and a controllable  
44 height of the knife (set at 100 µm). The plate was immersed in bi-distilled water for 15 mins at room  
45 temperature, for phase inversion. The PDO membrane was subsequently removed from the plate and  
46 freeze-dried.  
47  
48  
49  
50  
51  
52

53 The following step was the modification with gelatin, in order to improve the adhesion with the  
54 alginate/gelatin layers. The procedure was adapted from a previous paper [19]. An alkaline hydrolysis  
55 treatment was performed on the PDO membrane, by immersion in a 0.025 M sodium hydroxide  
56 solution for 3 mins, at room temperature. During the reaction, the membrane was maintained  
57  
58  
59  
60

1  
2  
3 suspended inside the solution, in order to treat both surfaces. After hydrolysis, the membrane was  
4 immersed in 0.01 mol/L HCl for 2.5 mins, for the acidification of COO<sup>-</sup> groups. The PDO membrane  
5 bearing carboxylic groups was immersed into a buffer solution (pH = 5) containing an EDC/NHS  
6 mixture, with a 3:1 M ratio, at 4 °C for 3 h. After several washings in deionized water to remove  
7 unreacted compounds, the PDO membrane was cut in a circular shape to fit the Petri dish and dipped  
8 in a 2% w/v solution of gelatin in bi-distilled water.  
9

10  
11  
12  
13  
14  
15  
16  
17 Alginate and gelatin were separately dissolved in bi-distilled water, at a concentration of 10% w/v, at  
18 50°C. Adequate volumes of the two solutions were mixed to obtain a blend with a 20:80 weight ratio  
19 between alginate and gelatin, in order to mimic the composition of the cardiac ECM [7, 8].  
20

21  
22  
23  
24 Half volume of the blend was poured into a Petri dish and cooled for 30 mins at room temperature.  
25  
26 The gelatin-treated PDO membrane was then positioned over the alginate/gelatin solution and the  
27 remaining blend was poured over the PDO membrane. The Petri dish was introduced into a freeze-  
28 drier. Freezing of the sample was performed at -25°C, followed by lyophilization using a ΔT of 10°C.  
29  
30  
31  
32  
33 The obtained sponge was cross-linked by a double treatment: i) exposure to GTA vapors, for the  
34 cross-linking of gelatin and ii) immersion in a solution of calcium ions, for the ionic cross-linking of  
35 alginate, as described in a previous paper [8].  
36  
37  
38

39  
40 At the end of the cross-linking procedure, the scaffold was washed thrice with bi-distilled water, to  
41 remove traces of GTA and excess calcium ions, then freeze-dried again.  
42  
43  
44  
45

### 46 47 *2.3 Scaffold functionalization*

48  
49 The first step of the functionalization procedure was the biotinylation of the scaffold, by dipping into  
50 a solution of biotinylated gelatin. Biotinylated gelatin was dissolved in bi-distilled water and a known  
51 volume of the solution was put in contact with the scaffold for 15 mins, until complete adsorption, in  
52 order to have 0.25 mg of biotinylated gelatin for each mg of gelatin in the scaffold.  
53  
54  
55

56  
57  
58 After freeze-drying, biotinylated gelatin adsorbed on the scaffold was cross-linked by treatment with  
59 a solution of EDC in acetone/water 90/10 for 24 h. A quantity of EDC corresponding to 30% of  
60

1  
2  
3 weight of biotinylated gelatin was used. The scaffold was washed thrice in bi-distilled water and then  
4  
5 the freeze-drying process was repeated.  
6

7  
8 The second step was the treatment with avidin. Avidin was dissolved in PBS at a concentration of 0.5  
9  
10 mg/ml. The scaffold was immersed in 5 ml of avidin solution, until complete adsorption, washed  
11  
12 thrice with bi-distilled water, to remove unlinked avidin, and then freeze-dried again.  
13

14  
15 The third step was the immobilization of biotinylated IGF-1 on the scaffold exposing avidin. The  
16  
17 growth factor was dissolved in bi-distilled water and a known volume of the growth factor solution  
18  
19 was adsorbed for 30 minutes at room temperature on the scaffold. For cell culture tests, two different  
20  
21 IGF-1 concentrations were tested: 5.6  $\mu\text{g/ml}$  and 10  $\mu\text{g/ml}$ . Samples were then washed thrice with bi-  
22  
23 distilled water to remove eventual unbound growth factor and the washing solutions were analysed  
24  
25 spectrophotometrically in order to quantify the real amount of growth factor immobilized onto the  
26  
27 scaffold surface.  
28  
29

30  
31 A final freeze-drying process was performed on the functionalized scaffolds.  
32  
33

#### 34 35 *2.4 Morphological analysis* 36

37  
38 Morphological analysis of both PDO-reinforced sponge and PDO membrane was performed by  
39  
40 scanning electron microscopy (SEM), using the microscope JSM 5600 (Jeol Ltd., Tokyo, Japan).  
41  
42 SEM images were also analyzed by the ImageJ software (National Institutes of Health) to determine  
43  
44 average pore dimension and porosity percentage. The percentage of porosity was calculated from the  
45  
46 ratio between the total pore area and the total scaffold area.  
47  
48  
49  
50

#### 51 52 *2.5 Infrared Chemical Imaging analysis* 53

54  
55 Infrared analysis was performed with a Fourier transformed infrared (FT-IR) Spectrometer (Spectrum  
56  
57 Spotlight 350 FT-NIR imaging system, Perkin Elmer, Waltham, MA, USA). The analysis was  
58  
59 performed in attenuated total reflectance (ATR) mode. The penetration depth was less than 1  $\mu\text{m}$  and  
60  
the spectral resolution was 4  $\text{cm}^{-1}$ .



1  
2  
3 Spectral images were acquired, using the infrared imaging system and analysed according to  
4  
5 previously described procedures [8].  
6

7 Near infrared (NIR) images in the range 7000-4000  $\text{cm}^{-1}$  were also acquired in order to investigate  
8  
9 the growth factor distribution.  
10  
11  
12  
13

## 14 2.6 Mechanical analysis

15  
16 The characterization of the viscoelastic properties of the scaffolds was carried out using a dynamic  
17  
18 mechanical analyser (DMA8000, Perkin-Elmer, Waltham, MA, USA), following the protocol  
19  
20 described in our previous paper [8]. Before analysis, samples were equilibrated for 3 h in a solution  
21  
22 simulating body fluids, at 37°C. Storage modulus ( $E'$ ), loss modulus ( $E''$ ) and tangent delta ( $\tan \delta$ )  
23  
24 were evaluated.  
25  
26  
27  
28  
29

## 30 2.7 Swelling test

31  
32 The swelling properties of the scaffolds were evaluated exposing them to aqueous vapour at 37°C,  
33  
34 following a standard procedure [8]. At appointed times, swelling percentage was evaluated according  
35  
36 to the following equation:  $(W_s - W_d) / W_d \times 100$ , where  $W_d$  is the starting dry weight and  $W_s$  is the  
37  
38 swollen weight.  
39  
40  
41  
42  
43  
44

## 45 2.8 Permeability test

46  
47 A permeation cell was used to test the permeability of the scaffolds to bi-distilled water, inducing a  
48  
49 flux through the scaffolds when subjected to a given pressure difference, as described in a previous  
50  
51 paper [20].  
52

53  
54 The following parameters were calculated:  
55

56  
57 
$$L_p = \frac{J_v}{\Delta P}$$
  
58 Hydraulic permeability ( $\text{cm}^2 \times \text{s} / \text{kg}$ )  
59

60 
$$K = \mu \cdot S \cdot \Delta P$$
  
Intrinsic permeability (from Darcy law, measured in  $\mu\text{m}^2$ )

1  
2  
3 where  $\mu$  is the viscosity of the solvent and  $S$  is the thickness of the scaffold.  
4  
5  
6

## 7 8 *2.9 Suturability test*

9  
10 A test to evaluate the suturability of the produced scaffolds was performed following a procedure  
11 described in literature [9]. Briefly, samples were cut to obtain rectangular strips (length 40 mm, width  
12 15 mm). A single 5–0 monofilament polyglyconate (Maxon™) suture was created 5 mm from the  
13 short edge of each sample and secured to a hook connected to a dynamometer (PCE group). An  
14 extension rate of 2 mm/s was used to pull the suture. Scaffolds were tested both in dry and in wet  
15 state, after equilibration for 15 mins in bi-distilled water. Suture retention force was considered to be  
16 the maximum force recorded by the dynamometer prior to pull-through of the suture.  
17  
18  
19  
20  
21  
22  
23  
24  
25  
26  
27

## 28 29 *2.10 In vitro study*

### 30 31 *2.10.1 Rat Cardiac progenitor Cells (rCPCs) isolation and culture*

32 rCPCs were isolated from green Fluorescence positive (GFP<sup>pos</sup>) rats [21] and cultured as previously  
33 described [18, 22]. rCPCs at passage 3 and 4 (P3-P4) were employed for the experiments carried on  
34 in this study.  
35  
36  
37  
38

### 39 40 *2.10.2 DiI cell labeling*

41 In order to detect rCPCs cultured on the scaffold, cells were stained before seeding with CellTracker  
42 CM-DiI (Invitrogen, C-7001) according to a previously described methodology [23].  
43  
44  
45

### 46 47 *2.10.3 Cell culture on PDO reinforced alginate/gelatin scaffolds*

48 Alginate/gelatin scaffolds reinforced with PDO were cut to fit exactly the size of one well of 8 well  
49 chamber slides (BD, USA). Samples were sterilized by UV exposure for 15 min on each side, as we  
50 already did with alginate/gelatin films [7] and scaffolds [8]. UV irradiation is commonly used in  
51 literature for scaffold sterilization and a low risk of material properties alterations is reported for  
52 exposure times below 2 h [24]. After sample sterilization, DiI labeled rCPCs were counted and seeded  
53 at  $45 \times 10^3$  cells/cm<sup>2</sup> density onto scaffolds containing 0.9  $\mu\text{g}/\text{cm}^2$  or 1.6  $\mu\text{g}/\text{cm}^2$  concentrations of  
54  
55  
56  
57  
58  
59  
60

1  
2  
3 IGF-1. Cells cultured on scaffolds without IGF-1 were considered as control. Cell loaded membranes  
4  
5 were evaluated 2, 7 and 14 days after cell plating. Quantification of cell adhesion was performed by  
6  
7 “Image Pro Plus 4.0” software as previously described [23].  
8

#### 9 10 *2.10.4 SEM analysis of cell seeding*

11  
12 In a subset of experiments, SEM analysis of rCPCs cultured for 14 days on alginate/gelatin scaffolds  
13  
14 was performed. Briefly, after fixation with paraformaldehyde, samples were dehydrated and critically  
15  
16 treated with 72 atm pCO<sub>2</sub> at 37 °C; the control and IGF-1 functionalized scaffolds were mounted on  
17  
18 metal stubs and coated with gold to a thickness of 60 nm using a gold sputter and analyzed by SEM  
19  
20 (Philips SEM 501, Eindhoven, The Netherlands).  
21  
22

#### 23 24 25 26 *2.11 In vivo study*

27  
28 In order to test the *in vivo* properties of functionalized alginate/gelatin scaffolds reinforced with PDO,  
29  
30 experiments were performed on a cryoinjury (CI) rat model. In particular, suturability, cell adhesion  
31  
32 to the scaffolds and myocardial remodeling were evaluated.  
33

34  
35 The study population consisted of male Wistar rats (*Rattus norvegicus*, Charles River, Italy) bred at  
36  
37 the University of Parma departmental animal facility, weighing 230-280 g (BW).  
38

39  
40 The investigation was approved by the Veterinary Animal Care and Use Committee of the University  
41  
42 of Parma and conformed to the National Ethical Guidelines (Italian Ministry of Health; D.L.vo 116,  
43  
44 January 27, 1992) and the Guide for the Care and Use of Laboratory Animals (NIH publication no.  
45  
46 85–23, revised 1996).  
47

48  
49 *In vivo* studies in the CI model were performed employing alginate/gelatin scaffolds reinforced with  
50  
51 PDO and functionalized with IGF-1 (0.9µg/cm<sup>2</sup>). rCPC-seeded (Alginate/Gelatin/PDO + IGF-1 +  
52  
53 rCPCs; n=4) or unseeded (Alginate/Gelatin/PDO + IGF-1; n=4) configurations were tested.  
54

55  
56 An additional group was represented by cryoinjured animals (Alginate/Gelatin/PDO + rCPCs; n=4)  
57  
58 in which rCPC seeded alginate/gelatin scaffolds in the absence of IGF-1 were applied.  
59  
60

1  
2  
3 Cell seeding was performed as previously described in “*in vitro study*”. After 2 days,  
4  
5 alginate/Gelatin/PDO + rCPCs were surgically sutured to cover the damaged area of the rat hearts.  
6  
7 Control groups (CTRL) were represented by animals subjected to myocardial damage without  
8  
9 scaffolds application.  
10

### 11 12 *2.11.1 Surgical procedure*

13  
14 The surgical procedure and the subsequent macroscopic examination of the rat myocardium were  
15  
16 performed according to a methodology well established in our laboratory and detailed in several  
17  
18 publications [16, 17, 25].  
19

20  
21 Briefly, rats were anesthetized with a combination of ketamine (40 mg/kg, i.p, Imalgene, Merial,  
22  
23 Milano, Italy) and Medetomidine Hydrochloride (0.15 mg/kg i.p., Domitor, Pfizer Italia S.r.l., Latina,  
24  
25 Italy), and artificially ventilated (tidal volume: 8–9  $\mu$ l/g; stroke rate: 165/min).  
26

27  
28 An incision was made at the left fourth intercostal space and cryoinjury was induced punching the  
29  
30 epicardium by a 20-gauge copper needle freshly immersed in liquid nitrogen.  
31

32  
33 In each experimental group, scaffolds were sutured with 7-0 silk surgical thread in correspondence to  
34  
35 the damaged area.  
36

37  
38 Sacrifice was performed at 10 days after CI. Rats were anesthetized as previously described and their  
39  
40 Body Weight recorded.  
41

42  
43 The heart of anesthetized animals was arrested in diastole by injection of 5 ml of cadmium chloride  
44  
45 (100 mmol/l iv) and briefly perfused at physiological mean arterial blood pressure with heparinized  
46  
47 PBS, followed by perfusion with 10% of formalin solution.  
48

### 49 50 *2.11.2 Cardiac Anatomy*

51  
52 The heart was excised and fixed for 24 h in 10% formalin, and the right ventricle (RV) and the left  
53  
54 ventricle (LV), including the septum, were separately weighed. The major cavitory axis of the LV  
55  
56 was measured from the aortic valve to the apex under a stereomicroscope with a ruler calibrated  
57  
58 exactly to 0.1  $\mu$ m (2Biological Instruments). Subsequently, the LV was sliced in three 3 mm thick  
59  
60 transverse sections corresponding respectively to the base, equatorial portion, and apex. On the

1  
2  
3 equatorial section, LV wall thickness and LV chamber diameter were measured using software for  
4 image analysis (Image Pro-plus, version 4.0; Media Cybernetics, USA). LV chamber volume was  
5  
6 calculated according to the Dodge equation, which equalizes the ventricular cavity to an ellipsoid  
7  
8  
9  
10 [26].

11  
12 Finally, the basal, equatorial, and apical sections were embedded in paraffin, and 5- $\mu$ m-thick sections  
13  
14 were cut for morphometric and immunohistochemical studies.

### 15 16 17 *2.11.3 Immunohistochemical analysis*

18  
19 The adhesion of GFP<sup>pos</sup> rCPCs seeded on scaffolds was determined by immunohistochemistry.

20  
21 GFP was detected by immunofluorescence. For this purpose, LV sections from different experimental  
22  
23 groups were incubated with primary antibody (polyclonal goat anti-GFP, dilution 1:100, Abcam,  
24  
25 UK). FITC-conjugated specific secondary antibody was used to detect the epitope. Nuclei were  
26  
27 recognized by the blue fluorescence of 4',6-diamidino-2-phenylindole (DAPI, Sigma) staining.  
28  
29 Immunostained sections were analyzed under a fluorescence microscope (Leica DMI6000B) in order  
30  
31 to compute the number of GFP<sup>pos</sup> rCPCs per mm<sup>2</sup> of myocardium.  
32  
33  
34  
35  
36

### 37 38 *2.12 Data management and statistics*

39  
40 The SPSS statistical package was used (SPSS, Chicago, IL, USA). Statistics of variables included  
41  
42 mean  $\pm$  standard error (S.E.M.), paired Student t-test, one- way analysis of variance (post-hoc  
43  
44 analyses: Tukey test or Holm-Sidak test, when appropriate). Statistical significance was set at  $p < 0.05$ ,  
45  
46  $p < 0.01$  and  $p < 0.001$ .  
47  
48  
49  
50

## 51 **3. Results and Discussion**

### 52 53 *3.1 Morphological analysis*

54  
55 The aim of SEM analysis was to investigate the morphological properties of the produced scaffolds,  
56  
57 especially in terms of porosity (pores dimension and interconnectivity), which can influence the  
58  
59 interactions between scaffold and cells, as well as scaffold infiltration by nerves and capillaries and  
60

1  
2  
3 the transport of nutrients necessary for cell metabolism. Moreover, morphological analysis was  
4 carried out to verify the adhesion of the PDO membrane to the alginate/gelatin layers, as well as to  
5 investigate any change in the alginate/gelatin sponge morphology after PDO inclusion.  
6  
7

8  
9  
10 SEM analysis was performed on PDO membrane and PDO reinforced alginate/gelatin sponges (figure  
11 2). Images were acquired on sample surface (figure 2a, 2c) and on sample section (figure 2b, 2d).

12  
13  
14 As shown by SEM micrographs, the PDO membrane presented a microporous surface skin (figure  
15 2a), while its section (figure 2b) was characterized by the presence of fingers, delimited by  
16 microporous walls. Fingers are normally obtained when a rapid phase inversion is carried out [27].

17  
18  
19 The alginate/gelatin sponge showed a porous structure, with pores of different sizes (figure 2c-d).

20  
21  
22 According to the typical morphology of sponges obtained by freeze-drying [8], pores were  
23 characterized by a good interconnectivity. The presence of the PDO membrane did not alter the  
24 morphology of the two external layers of alginate/gelatin sponge (figure 2d) whose structure in not  
25 reinforced alginate/gelatin sponges was previously documented [8]. Moreover, PDO membrane  
26 properly adhered to the alginate/gelatin sponge, as no sites of detachment between the sponge and the  
27 synthetic membrane were observed by SEM.  
28  
29

30  
31  
32 Pore size and porosity percentage were quantified analyzing SEM images by Image J software. The  
33 PDO membrane had pores with an average diameter of  $6 \pm 1 \mu\text{m}$  and the porosity percentage,  
34 calculated from the ratio between pores area and total area, was  $21.7 \pm 3.3 \%$ . Pores of PDO reinforced  
35 alginate/gelatin scaffold had an average diameter of  $139 \pm 37 \mu\text{m}$  and the porosity percentage was  
36  $55.1 \pm 10.3 \%$ . In a previous report on not reinforced alginate/gelatin scaffolds, we obtained pores  
37 with an average diameter of  $198 \pm 58 \mu\text{m}$  and a porosity percentage of  $60 \%$ , while the same  
38 parameters measured on decellularized myocardial tissue were, respectively,  $56 \pm 10 \mu\text{m}$  and  $13\%$   
39 [8]. Thus, no significant variations in terms of porosity were observed with respect to not reinforced  
40 alginate/gelatin scaffolds. However, the reinforced scaffolds developed in this work showed a higher  
41 porosity with respect to the native tissue, which may exert a positive effect on promoting both cells  
42  
43  
44  
45  
46  
47  
48  
49  
50  
51  
52  
53  
54  
55  
56  
57  
58  
59  
60  
61  
62  
63  
64  
65  
66  
67  
68  
69  
70  
71  
72  
73  
74  
75  
76  
77  
78  
79  
80  
81  
82  
83  
84  
85  
86  
87  
88  
89  
90  
91  
92  
93  
94  
95  
96  
97  
98  
99  
100  
101  
102  
103  
104  
105  
106  
107  
108  
109  
110  
111  
112  
113  
114  
115  
116  
117  
118  
119  
120  
121  
122  
123  
124  
125  
126  
127  
128  
129  
130  
131  
132  
133  
134  
135  
136  
137  
138  
139  
140  
141  
142  
143  
144  
145  
146  
147  
148  
149  
150  
151  
152  
153  
154  
155  
156  
157  
158  
159  
160  
161  
162  
163  
164  
165  
166  
167  
168  
169  
170  
171  
172  
173  
174  
175  
176  
177  
178  
179  
180  
181  
182  
183  
184  
185  
186  
187  
188  
189  
190  
191  
192  
193  
194  
195  
196  
197  
198  
199  
200  
201  
202  
203  
204  
205  
206  
207  
208  
209  
210  
211  
212  
213  
214  
215  
216  
217  
218  
219  
220  
221  
222  
223  
224  
225  
226  
227  
228  
229  
230  
231  
232  
233  
234  
235  
236  
237  
238  
239  
240  
241  
242  
243  
244  
245  
246  
247  
248  
249  
250  
251  
252  
253  
254  
255  
256  
257  
258  
259  
260  
261  
262  
263  
264  
265  
266  
267  
268  
269  
270  
271  
272  
273  
274  
275  
276  
277  
278  
279  
280  
281  
282  
283  
284  
285  
286  
287  
288  
289  
290  
291  
292  
293  
294  
295  
296  
297  
298  
299  
300  
301  
302  
303  
304  
305  
306  
307  
308  
309  
310  
311  
312  
313  
314  
315  
316  
317  
318  
319  
320  
321  
322  
323  
324  
325  
326  
327  
328  
329  
330  
331  
332  
333  
334  
335  
336  
337  
338  
339  
340  
341  
342  
343  
344  
345  
346  
347  
348  
349  
350  
351  
352  
353  
354  
355  
356  
357  
358  
359  
360  
361  
362  
363  
364  
365  
366  
367  
368  
369  
370  
371  
372  
373  
374  
375  
376  
377  
378  
379  
380  
381  
382  
383  
384  
385  
386  
387  
388  
389  
390  
391  
392  
393  
394  
395  
396  
397  
398  
399  
400  
401  
402  
403  
404  
405  
406  
407  
408  
409  
410  
411  
412  
413  
414  
415  
416  
417  
418  
419  
420  
421  
422  
423  
424  
425  
426  
427  
428  
429  
430  
431  
432  
433  
434  
435  
436  
437  
438  
439  
440  
441  
442  
443  
444  
445  
446  
447  
448  
449  
450  
451  
452  
453  
454  
455  
456  
457  
458  
459  
460  
461  
462  
463  
464  
465  
466  
467  
468  
469  
470  
471  
472  
473  
474  
475  
476  
477  
478  
479  
480  
481  
482  
483  
484  
485  
486  
487  
488  
489  
490  
491  
492  
493  
494  
495  
496  
497  
498  
499  
500  
501  
502  
503  
504  
505  
506  
507  
508  
509  
510  
511  
512  
513  
514  
515  
516  
517  
518  
519  
520  
521  
522  
523  
524  
525  
526  
527  
528  
529  
530  
531  
532  
533  
534  
535  
536  
537  
538  
539  
540  
541  
542  
543  
544  
545  
546  
547  
548  
549  
550  
551  
552  
553  
554  
555  
556  
557  
558  
559  
560  
561  
562  
563  
564  
565  
566  
567  
568  
569  
570  
571  
572  
573  
574  
575  
576  
577  
578  
579  
580  
581  
582  
583  
584  
585  
586  
587  
588  
589  
590  
591  
592  
593  
594  
595  
596  
597  
598  
599  
600  
601  
602  
603  
604  
605  
606  
607  
608  
609  
610  
611  
612  
613  
614  
615  
616  
617  
618  
619  
620  
621  
622  
623  
624  
625  
626  
627  
628  
629  
630  
631  
632  
633  
634  
635  
636  
637  
638  
639  
640  
641  
642  
643  
644  
645  
646  
647  
648  
649  
650  
651  
652  
653  
654  
655  
656  
657  
658  
659  
660  
661  
662  
663  
664  
665  
666  
667  
668  
669  
670  
671  
672  
673  
674  
675  
676  
677  
678  
679  
680  
681  
682  
683  
684  
685  
686  
687  
688  
689  
690  
691  
692  
693  
694  
695  
696  
697  
698  
699  
700  
701  
702  
703  
704  
705  
706  
707  
708  
709  
710  
711  
712  
713  
714  
715  
716  
717  
718  
719  
720  
721  
722  
723  
724  
725  
726  
727  
728  
729  
730  
731  
732  
733  
734  
735  
736  
737  
738  
739  
740  
741  
742  
743  
744  
745  
746  
747  
748  
749  
750  
751  
752  
753  
754  
755  
756  
757  
758  
759  
760  
761  
762  
763  
764  
765  
766  
767  
768  
769  
770  
771  
772  
773  
774  
775  
776  
777  
778  
779  
780  
781  
782  
783  
784  
785  
786  
787  
788  
789  
790  
791  
792  
793  
794  
795  
796  
797  
798  
799  
800  
801  
802  
803  
804  
805  
806  
807  
808  
809  
810  
811  
812  
813  
814  
815  
816  
817  
818  
819  
820  
821  
822  
823  
824  
825  
826  
827  
828  
829  
830  
831  
832  
833  
834  
835  
836  
837  
838  
839  
840  
841  
842  
843  
844  
845  
846  
847  
848  
849  
850  
851  
852  
853  
854  
855  
856  
857  
858  
859  
860  
861  
862  
863  
864  
865  
866  
867  
868  
869  
870  
871  
872  
873  
874  
875  
876  
877  
878  
879  
880  
881  
882  
883  
884  
885  
886  
887  
888  
889  
890  
891  
892  
893  
894  
895  
896  
897  
898  
899  
900  
901  
902  
903  
904  
905  
906  
907  
908  
909  
910  
911  
912  
913  
914  
915  
916  
917  
918  
919  
920  
921  
922  
923  
924  
925  
926  
927  
928  
929  
930  
931  
932  
933  
934  
935  
936  
937  
938  
939  
940  
941  
942  
943  
944  
945  
946  
947  
948  
949  
950  
951  
952  
953  
954  
955  
956  
957  
958  
959  
960  
961  
962  
963  
964  
965  
966  
967  
968  
969  
970  
971  
972  
973  
974  
975  
976  
977  
978  
979  
980  
981  
982  
983  
984  
985  
986  
987  
988  
989  
990  
991  
992  
993  
994  
995  
996  
997  
998  
999  
1000

### 3.2 Infrared Chemical Imaging analysis

Infrared analysis was performed on the scaffolds, at different steps of the preparation procedure, in order to verify the efficacy of the performed chemical treatments.

Infrared spectra were acquired for the PDO membrane, before and after the hydrolysis treatment, as well as after dipping in gelatin. As shown in figure 3a, PDO spectrum peaked at  $1740\text{ cm}^{-1}$ , due to C=O. Basic hydrolysis of PDO determined the cleavage of the ester bonds, with the formation of  $\text{COO}^-$  groups (at  $1600\text{ cm}^{-1}$ ). After dipping in gelatin, the presence of the protein was shown by the typical absorption peaks due to Amide I (at  $1630\text{ cm}^{-1}$ ) and Amide II (at  $1539\text{ cm}^{-1}$ ).

In order to investigate the distribution of the protein on the membrane, the chemical map as a function of the ratio between the band at  $1780\text{-}1714\text{ cm}^{-1}$  (due to PDO) and the band at  $1714\text{-}1595\text{ cm}^{-1}$  (due to gelatin) was elaborated (figure 3b). The value of the band ratio (2.7) was almost constant on all the analysed surface, demonstrating a homogeneous distribution of gelatin.

Chemical Imaging analysis was also performed on a section of the reinforced scaffold, in a region close to the PDO membrane, to eventually point out changes induced by the presence of the synthetic membrane. The Chemical map is shown in figure 3c. The presence of the PDO membrane was demonstrated by a nearly  $100\text{ }\mu\text{m}$  thick layer. The spectra acquired in this region were characterized by the presence of the typical PDO absorption band at  $1740\text{ cm}^{-1}$ , while the spectra acquired in the region around the PDO membrane showed the typical absorption peaks of the two natural polymers:  $1640\text{ cm}^{-1}$ , due to gelatin Amide I;  $1544\text{ cm}^{-1}$ , due to gelatin Amide II and  $1034\text{ cm}^{-1}$ , due alginate C-O-C (figure 3d). These results suggested that PDO did not alter the chemical properties of the natural polymer blend. In particular, the displacement of the typical absorption peaks, with respect to pure alginate (C-O-C =  $1027\text{ cm}^{-1}$ ) and pure gelatin (Amide I =  $1630\text{ cm}^{-1}$  and Amide II =  $1539\text{ cm}^{-1}$ ), indicative of molecular interactions between the protein component and the polysaccharide component and previously observed in native sponges [8], were confirmed in PDO-reinforced sponges.

1  
2  
3 Chemical Imaging investigation in the near infrared region was performed to study the chemical  
4 modifications induced by dipping in biotinylated gelatin. NIR maps and spectra were acquired for  
5 alginate/gelatin/PDO sponges, before and after dipping (figure 4). All NIR spectra showed the  
6 presence of second overtone absorptions due to OH ( $5100\text{ cm}^{-1}$ ), NH ( $4600\text{ cm}^{-1}$ ) and CH ( $4378\text{ cm}^{-1}$ )  
7  $^1$ ). In the spectra acquired after dipping, we observed an intensification of NH absorption and the  
8 presence of two additional bands ( $5800\text{ cm}^{-1}$  and  $4800\text{ cm}^{-1}$ ), which can be attributed to biotin. In  
9 order to investigate biotin distribution, the chemical map in function of biotin absorption peak ( $4800$   
10  $\text{cm}^{-1}$ ) was elaborated (figure 4c). Spectra acquired in different points of the chemical map showed the  
11 presence of biotin absorption peak, demonstrating a homogeneous distribution of biotinylated gelatin  
12 on the sponge (figure 4d).

13  
14 Functionalized scaffolds were also characterized by chemical imaging analysis in  $\mu\text{ATR}$  mode, at  
15 different steps of the functionalization procedure. Chemical maps were acquired for biotinylated  
16 scaffold, pure avidin, biontinylated scaffold treated with avidin and scaffold functionalized with the  
17 biotinylated growth factor. The medium spectra recorded for each of the previous mentioned chemical  
18 maps are collected in figure 3e-h. All the acquired spectra were similar, being protein the main  
19 component. In particular, avidin spectrum (figure 3f) showed a characteristic absorption peak at  $1061$   
20  $\text{cm}^{-1}$ , undetectable in the biotinylated scaffold (figure 3e) while present in the avidin treated scaffold  
21 (figure 3g), demonstrating the good outcome of this procedure. After growth factor binding, the avidin  
22 peak intensity decreased, because of the presence of the bioactive molecule (figure 3h).

### 23 24 25 26 27 28 29 30 31 32 33 34 35 36 37 38 39 40 41 42 43 44 45 46 47 48 49 *3.3 Mechanical analysis*

50  
51 Mechanical properties of functionalized and not functionalized scaffolds were preliminary compared  
52 and no significant difference was found (data not shown). This result was expected, as there is no  
53 report in literature about the effect of growth factor immobilization on scaffold mechanical properties.  
54 Being not functionalized scaffolds significantly less expensive than the functionalized ones, complete  
55 investigation was performed on not functionalized scaffolds.



1  
2  
3 Results of the mechanical characterization, carried out by DMA, are collected in table 1.  
4

5 As expected, increasing the oscillation frequency, an increase was observed for values of  $E'$  and  $E''$ .  
6

7 This result demonstrated that the stiffness of alginate/gelatin/PDO scaffolds increased with frequency  
8  
9 increase. This stiffening involves both an increase in elasticity ( $E'$ ) and an increase in heat dissipation  
10  
11 ( $E''$ ). Values of  $\tan \delta$  did not show variations by increasing frequency, suggesting that  $E'$  and  $E''$   
12  
13 increased with frequency at the same proportion. Values of  $E'$  were more than one order of magnitude  
14  
15 higher than values of  $E''$ , with a  $\tan \delta$  equal to 0.04, and this result demonstrated the elastic behaviour  
16  
17 of the developed scaffolds. In a previous paper, the same DMA analysis was carried out on not  
18  
19 reinforced alginate/gelatin scaffolds and the values of  $E'$  and  $E''$  were at least one order of magnitude  
20  
21 smaller than those obtained in this work [8]. This result showed that the presence of the PDO  
22  
23 membrane increased the stiffness of the alginate/gelatin scaffolds. Reinforced scaffolds resulted also  
24  
25 stiffer than the native myocardium [8]. However, as reported in literature, a cardiac scaffold stiffer  
26  
27 than the surrounding tissue can favour a positive outcome in terms of reduction of infarct expansion,  
28  
29 attenuation of left ventricle remodeling, and amelioration of global left ventricle function [28].  
30  
31  
32  
33  
34  
35  
36  
37

### 38 *3.4 Swelling test*

39 Swelling test was performed to evaluate the ability of the obtained materials to absorb water, which  
40  
41 is related to the hydrophilicity degree and depends on several factors, including the chemical  
42  
43 properties of the materials used for scaffold preparation, the cross-linking degree, the interactions  
44  
45 between components and the morphological properties of the developed scaffolds.  
46  
47

48 The swelling kinetics for the alginate/gelatin/PDO scaffolds and for the PDO membrane are reported  
49  
50 in figure 5 and compared with that obtained for not reinforced alginate/gelatin scaffolds [8]. The PDO  
51  
52 membrane showed a low swelling degree, with a plateau of around 10% after 96 hours, in agreement  
53  
54 with the low hydrophilicity of the synthetic polymer [29]. For the alginate/gelatin/PDO scaffold, we  
55  
56 observed a rapid water uptake during the first hours, then water absorption gradually proceeded,  
57  
58 reaching a plateau of around 30% after 96 hours. Comparing these data with the swelling kinetics of  
59  
60

1  
2  
3 not reinforced alginate/gelatin scaffolds (swelling at plateau of around 67%, [8]), the presence of the  
4  
5 PDO membrane induced a significant reduction in water absorption, although maintaining a good  
6  
7 degree of hydrophilicity.  
8  
9

### 10 11 12 3.5 Permeability test 13

14 It is well known that one of the most important properties of the scaffolds for *in vitro* regeneration is  
15 their porosity and permeability, to provide cell growth nutrients transport and catabolites removal  
16  
17 [30]. If cell culture is carried out in static conditions, nutrient transport can be of diffusive type, while  
18  
19 with a cell culture in dynamic conditions based on the use of a bioreactor the transport might be of  
20  
21 both diffusive and convective kind.  
22  
23

24  
25 A permeability apparatus was used here to evaluate the hydraulic permeability ( $L_p$ ), which is a  
26  
27 quantitative index of the convective transport of a solution through a scaffold, and the coefficient  $K$ ,  
28  
29 called intrinsic permeability, which is dependent on the porosity of the scaffold. On the basis of the  
30  
31 order of magnitude of the calculated  $K$  value, it is possible to evaluate the permeability degree of the  
32  
33 membrane.  
34  
35

36  
37 Permeability tests were performed on not reinforced alginate/gelatin sponges, PDO membrane and  
38  
39 alginate/gelatin sponges reinforced with PDO. Calculated values of  $L_p$  and  $K$  are collected in table  
40  
41  
42 2.  
43

44 The obtained results showed that the introduction of the PDO membrane in the alginate/gelatin  
45  
46 sponge produced a significant decrease of  $L_p$  and  $K$  values, with respect to not reinforced scaffold.  
47  
48 Scaffold permeability, and in particular intrinsic permeability, is strictly connected to porosity and  
49  
50 pore interconnectivity [31]. As discussed in the morphological analysis section, PDO membrane  
51  
52 porosity was significantly lower than that of alginate/gelatin scaffold. Even if the presence of the  
53  
54 PDO membrane did not reduce the overall porosity of the scaffold, representing only a 100  $\mu\text{m}$  thick  
55  
56 layer over a total scaffold thickness of around 4 mm, a significant impact on scaffold permeability  
57  
58 was observed. However, values of permeability parameters obtained in PDO reinforced  
59  
60

alginate/gelatin scaffolds were comparable with those obtained for other scaffolds aiming at tissue engineering applications [32] and specifically applied to cardiac tissue [20].

### 3.6 Suturability test

Preformed three dimensional scaffolds for cardiac tissue engineering have to be implanted on the patient heart through a surgical procedure and their suture resistance is a fundamental parameter to avoid failures during implantation.

Results of suturability tests, performed on alginate/gelatin scaffolds with or without PDO reinforcement, under dry and wet conditions, are collected in table 3.

Obtained results showed that the introduction of the PDO membrane for scaffold reinforcement significantly increased the suture retention force of the alginate/gelatin scaffolds. This effect was particularly evident under wet conditions, where the assessment of suture retention force of not reinforced scaffolds was unfeasible due to a rapid rupture. Reference values of suture retention force for cardiovascular tissue are available in literature for human coronary artery ( $1.96 \pm 1.1$  N) and saphenous vein ( $1.92 \pm 0.02$  N) [33], while the suture retention force of a full thickness patch implanted in a human left ventricle was estimated equal to  $0.61 \pm 0.18$  N [34]. After inclusion of the PDO membrane, values of suture retention force of our scaffolds were above these limits, both under dry and wet conditions. Therefore, the reinforced scaffolds developed in this work can be considered adequate for the aimed application.

### 3.7 *In vitro* study

Cell culture tests were performed on PDO reinforced alginate/gelatin scaffolds, functionalized with two different concentrations of biotinylated IGF-1 ( $0.9 \mu\text{g}/\text{cm}^2$  and  $1.6 \mu\text{g}/\text{cm}^2$ ).

The evaluation of the presence of rCPCs two days after seeding revealed that higher concentrations of IGF-1 improved cell adhesion when compared to both IGF-1 free (2.67-fold increase) and  $0.9 \mu\text{g}/\text{cm}^2$  IGF-1 functionalized (6.64-fold increase) scaffolds. On the other hand, low IGF-1 dose

1  
2  
3 better preserved long term cell adhesion since at 14 days a 3.18-fold increase in rCPC number was  
4 documented compared to 2 days cell culture. The increase in rCPCs adhesion produced by IGF-1  
5 scaffold functionalization was also confirmed by SEM. On control scaffolds, round shaped cells  
6 weakly integrated with the membrane by few filopodia were observed (Figure 6a). Conversely, both  
7 doses of IGF-1 increased cell adhesion, promoted intercellular communication and full seeding of  
8 scaffolds by rCPCs (Figure 6b-c).  
9  
10  
11  
12  
13  
14  
15  
16  
17  
18

### 19 3.8 *In vivo* study

#### 20 3.8.1 Cardiac Anatomy

21 Based on *in vitro* findings, further *in vivo* studies were performed only on scaffolds containing 0.9  
22  $\mu\text{g}$  of IGF-1/cm<sup>2</sup>.  
23

24 The alginate/gelatin/PDO scaffolds did not significantly affect rat body and cardiac weights 10 days  
25 after cryoinjury (CI, data not shown).  
26

27 Application of alginate/gelatin/PDO scaffolds appeared to be able to reduce LV dilatation at 10 days  
28 after CI, although functionalization by IGF-1 did not result in an additive effect on this parameter.  
29 However, functionalized scaffolds seeded with rCPCs more effectively reduced LV dilatation, since  
30 a 1.33-fold decrease in chamber volume was measured at 10 days after surgical procedure compared  
31 to CTRL group (Table 4).  
32

#### 33 3.8.2 Immunohistochemical analysis

34 The evaluation of the number of GFP<sup>POS</sup> rCPCs present on alginate/gelatin/PDO scaffolds (Fig. 7a-b),  
35 documented cells retention to the scaffold after 10 days from CI. Importantly, functionalization with  
36 IGF-1 significantly increased by 1.35-fold ( $p=0.026$ ) the number of rCPCs within the  
37 alginate/gelatin/PDO scaffolds sutured to the damaged myocardium (Fig. 7c).  
38  
39  
40  
41  
42  
43  
44  
45  
46  
47  
48  
49  
50  
51  
52  
53  
54  
55  
56  
57

## 58 4. Conclusions

1  
2  
3 Here we report on a simple method to develop bioactive reinforced alginate/gelatin scaffolds. A  
4 microporous PDO membrane obtained by phase inversion was introduced within two alginate/gelatin  
5 sponge layers, producing a reinforced scaffold with improved mechanical properties and a resistance  
6 to suture adequate for surgical procedures. In addition to the introduction of the reinforcement  
7 membrane, the scaffolds were functionalized with biotinylated IGF-1, using the avidin-biotin binding  
8 strategy. *In vitro* and *in vivo* tests were performed on the produced prototypes. Overall, obtained  
9 results suggest that PDO reinforced alginate/gelatin sponges, decorated with biotinylated IGF-1,  
10 represent a promising system for promoting cardiac tissue regeneration.  
11

12 In particular, for what concerns scaffold functionalization, both cell culture tests and *in vivo* tests  
13 showed that scaffold decoration with biotinylated IGF-1 promoted cell retention and reduced LV  
14 dilatation. These findings suggest that the avidin-biotin binding system, used for the first time in this  
15 work for the modification of three-dimensional preformed scaffolds for cardiac tissue engineering, is  
16 an effective strategy for scaffold decoration. Combining this strategy with the use of different  
17 bioactive molecules, it could be possible to create a complex microenvironment, controlling the  
18 endogenous regeneration of the injured myocardium.  
19

20 With reference to scaffold reinforcement, results showed that the inclusion of the PDO membrane  
21 successfully improved the mechanical properties and the resistance to sutures of alginate/gelatin  
22 scaffolds. This achievement represents a significant step towards the clinical application of an  
23 engineered myocardial patch for the treatment of infarcted heart. However, the presence of the  
24 synthetic membrane partially reduced the hydrophilicity of the scaffold, as well as its permeability.  
25 Further investigations will aim at the design of different reinforcement structures, with a reduced  
26 impact on scaffold morphology and related properties, such as developing fiber-based support  
27 systems.  
28  
29  
30  
31  
32  
33  
34  
35  
36  
37  
38  
39  
40  
41  
42  
43  
44  
45  
46  
47  
48  
49  
50  
51  
52  
53  
54  
55  
56  
57  
58  
59  
60

1  
2  
3  
4  
5  
6  
7  
8  
9  
10  
11  
12  
13  
14  
15  
16  
17  
18  
19  
20  
21  
22  
23  
24  
25  
26  
27  
28  
29  
30  
31  
32  
33  
34  
35  
36  
37  
38  
39  
40  
41  
42  
43  
44  
45  
46  
47  
48  
49  
50  
51  
52  
53  
54  
55  
56  
57  
58  
59  
60

### **5. Acknowledgments**

This work was supported by the European Commission FP7 Programme, grant 214539.

For Peer Review

## References

- [1] Alwan A. *Global status report on noncommunicable diseases 2010*. Geneva: World Health Organization, 2011, pp. 176.
- [2] Miniati DN, Robbins RC. Heart transplantation: A thirty years perspective. *Annu Rev Med* 2002; 53: 189–205.
- [3] Zammaretti P, Jaconi M. Cardiac tissue engineering: Regeneration of the wounded heart. *Curr Opin Biotechnol* 2004; 15: 430–434.
- [4] Shapira A, Feiner R, Dvir T. Composite biomaterial scaffolds for cardiac tissue engineering. *Int Mater Rev* 2016; 61: 1-19.
- [5] Chen QZ, Harding SE, Ali NN, et al. Biomaterials in cardiac tissue engineering: Ten years of research survey. *Mater Sci Eng R* 2008; 59: 1-37.
- [6] Tallawi M, Rosellini E, Barbani N, et al. Strategies for the chemical and biological functionalization of scaffolds for cardiac tissue-engineering. A review. *J R Soc Interface* 2015; 12: 20150254.
- [7] Rosellini E, Cristallini C, Barbani N, et al. Preparation and characterization of alginate/gelatin blend films for cardiac tissue engineering. *J Biomed Mater Res A* 2009; 91A: 447-453.
- [8] Rosellini E, Zhang YS, Migliori B, et al. Protein/Polysaccharide-based Scaffolds Mimicking Native Extracellular Matrix for Cardiac Tissue Engineering Applications. *J Biomed Mater Res A* 2018; 106: 769-781.
- [9] Soletti L, Hong Y, Guan J, et al. A bilayered elastomeric scaffold for tissue engineering of small diameter vascular grafts. *Acta Biomater* 2010; 6: 110-122.
- [10] Berry AR, Wilson MC, Thomson JW, et al. Polydioxanone: A new synthetic absorbable suture. *J R Coll Surg Edinb* 1981; 26: 170-172.
- [11] Wilchek M, Bayer EA. Protein biotinylation. *Methods Enzymol* 1990; 184: 167-74.
- [12] Lchek M, Bayer E. Introduction to avidin–biotin technology. *Methods Enzym* 1990; 184: 5-13.

- 1  
2  
3 [13] Bhat VD, Klitzman B, Koger K, et al. Improving endothelial cell adhesion to vascular graft  
4 surfaces: clinical need and strategies. *J Biomater Sci Polym Ed* 1998; 9: 1117-1135.  
5  
6  
7 [14] Tsai W, Wang M. Effects of an avidin–biotin binding system on chondrocyte adhesion and  
8 growth on biodegradable polymers. *Macromol Biosci* 2005; 5: 214-221.  
9  
10  
11 [15] Davis ME, Hsieh PCH, Takahashi T, et al. Local myocardial insulin-like growth factor 1 (IGF-  
12 1) delivery with biotinylated peptide nanofibers improves cell therapy for myocardial infarction. *Proc*  
13 *Natl Acad Sci USA* 2006; 103: 8155-8160.  
14  
15  
16 [16] Rossini A, Frati C, Lagrasta C, et al. Human cardiac and bone marrow stromal cells exhibit  
17 distinctive properties related to their origin. *Cardiovasc Res* 2011; 89: 650-660.  
18  
19  
20 [17] Bocchi L, Savi M, Graiani G, et al. Growth Factor-Induced Mobilization of Cardiac Progenitor  
21 Cells Reduces the Risk of Arrhythmias, in a Rat Model of Chronic Myocardial Infarction. *PLoS One*  
22 2011; 6: e17750.  
23  
24  
25 [18] Frati C, Savi M, Graiani G, et al. Resident cardiac stem cells. *Curr Pharm Des* 2011; 17: 3252-  
26 3257.  
27  
28  
29 [19] Rosellini E, Cristallini C, Guerra GD, et al. Surface chemical immobilization of bioactive  
30 peptides on bioresorbable synthetic polymers for cardiac tissue engineering. *J Biomater Sci Polym*  
31 *Ed* 2015; 26: 515-533.  
32  
33  
34 [20] Rai R, Tallawi M, Frati C, et al. Bioactive electrospun fibers of poly(glycerol sebacate) and  
35 poly( $\epsilon$ -caprolactone) for cardiac patch application. *Adv Healthc Mater* 2015; 4: 2012-2025.  
36  
37  
38 [21] Okabe M, Ikawa M, Kominami K, et al. 'Green mice' as a source of ubiquitous green cells. *FEBS*  
39 *Lett* 1997; 407: 313-319.  
40  
41  
42 [22] Giuliani A, Frati C, Rossini A, et al. High-resolution X-ray microtomography for three-  
43 dimensional imaging of cardiac progenitor cell homing in infarcted rat hearts. *J Tissue Eng Regen*  
44 *Med* 2011; 5: e168-e178.  
45  
46  
47 [23] Rai R, Tallawi M, Barbani N, et al. Biomimetic poly(glycerol sebacate) (PGS) membranes for  
48 cardiac patch application. *Mater Sci Eng C Mater Biol Appl* 2013; 33: 3677-3687.  
49  
50  
51  
52  
53  
54  
55  
56  
57  
58  
59  
60



- [24] Dai Z, Ronholm J, Tian Y, et al. Sterilization techniques for biodegradable scaffolds in tissue engineering applications. *J Tissue Eng* 2016; 7: 1-13.
- [25] Savi M, Bocchi L, Rossi S, et al. Antiarrhythmic effect of growth factor-supplemented cardiac progenitor cells in chronic infarcted heart. *Am J Physiol Heart Circ Physiol* 2016; 310: H1622-H1648.
- [26] Dodge HT, Baxley WA. Left ventricular volume and mass and their significance in heart disease. *Am J Cardiol* 1969; 23: 528-537.
- [27] Strathmann H, Kock K. The formation mechanism of phase inversion membranes. *Desalination* 1977; 21: 241-255.
- [28] Morita M, Eckert C, Matsuzaki K. Modification of infarct material properties limits adverse ventricular remodeling. *Ann Thorac Surg* 2011; 92: 617-624.
- [29] Nair LS, Laurencin CT. Biodegradable polymers as biomaterials. *Prog Polym Sci* 2007; 32: 762-798.
- [30] Karande TS, Ong JL and Agrawal CM. Diffusion in Musculoskeletal Tissue Engineering Scaffolds: Design Issues Related to Porosity, Permeability, Architecture, and Nutrient Mixing. *Ann Biomed Eng* 2004; 32: 1728–1743.
- [31] Pennella F, Cerino G, Massai D, et al. A Survey of Methods for the Evaluation of Tissue Engineering Scaffold Permeability. *Ann Biomed Eng* 2013; 41: 2027–2041.
- [32] Sell S, Barnes C, Simpson D, et al. Scaffold permeability as a means to determine fiber diameter and pore size of electrospun fibrinogen. *J Biomed Mater Res A* 2008; 85:115–126.
- [33] l'Heureux N, Dusserre N, Konig G, et al. Human tissue-engineered blood vessels for adult arterial revascularization. *Nat Med* 2006; 12: 361-365.
- [34] Pok S, Myers JD, Madhally SV, et al. A multilayered scaffold of a chitosan and gelatin hydrogel supported by a PCL core for cardiac tissue engineering. *Acta Biomater* 2013; 9: 5630–5642.

1  
2  
3 **Tables**  
4  
5  
6  
7

8  
9  
10  
11  
12  
13  
14  
15  
16

	E' (MPa)	E'' (MPa)	Tan $\delta$
1 Hz	7.67 $\pm$ 0.01	0.28 $\pm$ 0.01	0.04 $\pm$ 0.01
3.5 Hz	7.90 $\pm$ 0.01	0.31 $\pm$ 0.02	0.04 $\pm$ 0.01
10 Hz	7.99 $\pm$ 0.01	0.34 $\pm$ 0.03	0.04 $\pm$ 0.01

17 **Table 1.** Storage modulus (E'), loss modulus (E'') and tan delta of alginate/gelatin/PDO sponges,  
18 measured by DMA at three different frequencies (1, 3.5 and 10 Hz).  
19  
20  
21  
22

23  
24  
25  
26  
27  
28  
29  
30  
31  
32

	Lp (cm $\times$ s <sup>-1</sup> $\times$ Pa <sup>-1</sup> )	K ( $\mu$ m <sup>2</sup> )
Alginate/Gelatin	3.5 $\times$ 10 <sup>-6</sup>	2.5 $\times$ 10 <sup>-2</sup>
PDO	4.0 $\times$ 10 <sup>-8</sup>	1.1 $\times$ 10 <sup>-4</sup>
Alginate/Gelatin/PDO	6.5 $\times$ 10 <sup>-7</sup>	2.0 $\times$ 10 <sup>-3</sup>

33 **Table 2.** Values of Lp and K, calculated for alginate/gelatin sponge, PDO membrane, alginate/gelatin  
34 sponge reinforced with PDO.  
35  
36  
37  
38  
39

40  
41  
42  
43  
44  
45  
46  
47  
48  
49

	Suture retention force (N)	
	Dry Conditions	Wet conditions
Alginate/Gelatin	16.2 $\pm$ 0.3	n.d.
Alginate/Gelatin/PDO	24.4 $\pm$ 0.3	4.3 $\pm$ 1.3

50 **Table 3.** Values of suture retention force measured under dry and wet conditions for alginate/gelatin  
51 and alginate/gelatin/PDO scaffolds.  
52  
53  
54  
55  
56  
57  
58  
59  
60

	Chamber Volume, mm <sup>3</sup> (Mean ± St.Dev.)
<b>CTRL</b>	360.01 ± 32.85
<b>Alginate/Gelatin/PDO + rCPCs</b>	278.78 ± 52.79
<b>Alginate/Gelatin/PDO + IGF-1</b>	296.28 ± 19.99
<b>Alginate/Gelatin/PDO + IGF-1 + rCPCs</b>	271.08 ± 72.78

**Table 4.** Measurements of Left Ventricular (LV) chamber volume in different experimental groups 10 days after cryoinjury. **CTRL:** cryoinjured rat in the absence of scaffolds; **IGF-1:** Insulin-like Growth Factor 1; **rCPCs:** rat Cardiac Progenitor Cells.

1  
2  
3 **Figure Legend**  
4

5 **Figure 1.** Schematic representation of the alginate/gelatin cardiac patch developed in this work,  
6 comprising: (i) reinforcement with PDO membrane, for improved suture resistance; (ii) IGF-1  
7 immobilization, through avidin-biotin binding strategy.  
8  
9

10  
11  
12 **Figure 2.** SEM micrographs of PDO membrane, (a) surface and (b) section; PDO reinforced  
13 alginate/gelatin scaffolds, (c) surface and (d) section.  
14

15  
16  
17 **Figure 3.** (a) Infrared spectra of untreated PDO, hydrolysed PDO and gelatin functionalized PDO;  
18 (b) Chemical map of PDO membrane functionalized with gelatin, in function of the band ratio  
19 between the band at 1780-1714  $\text{cm}^{-1}$  (due to PDO) and the band at 1714-1595  $\text{cm}^{-1}$  (due to gelatin);  
20 (c) Chemical map of alginate/gelatin sponge reinforced with PDO; (d) Spectra from the chemical map  
21 in (c). (e-h) Infrared medium spectra of: (e) biotinylated scaffold; (f) avidin; (g) scaffold treated with  
22 avidin and (h) scaffold functionalized with biotinylated growth factor.  
23  
24  
25  
26  
27  
28  
29

30  
31 **Figure 4.** (a) NIR spectra of not functionalized alginate/gelatin/PDO sponge; (b) NIR spectra of  
32 alginate/gelatin/PDO sponge, after dipping in biotinylated gelatin; (c) NIR chemical map in function  
33 of biotin absorption peak at 4800  $\text{cm}^{-1}$ ; (d) spectra acquired in different areas of the NIR chemical  
34 map.  
35  
36  
37  
38

39  
40 **Figure 5.** Swelling kinetic for PDO membrane and for alginate/gelatin/PDO scaffolds. Swelling test  
41 was performed by exposure to aqueous vapour. Results were compared with those obtained for not  
42 reinforced alginate/gelatin scaffolds [8].  
43  
44  
45

46  
47 **Figure 6.** SEM images of rCPCs two weeks after seeding on alginate/gelatin/PDO (a),  
48 alginate/gelatin/PDO + IGF-1 0.9  $\mu\text{g}/\text{cm}^2$  (b) and alginate/gelatin/PDO + IGF-1 1.6  $\mu\text{g}/\text{cm}^2$  (c). Scale  
49 bars: a=10 $\mu\text{m}$ , b and c=100 $\mu\text{m}$ .  
50  
51  
52

53  
54 **Figure 7.** Immunofluorescence detection of GFP<sup>POS</sup> rCPCs (Green) on alginate/gelatin/PDO (a) and  
55 alginate/gelatin/PDO + IGF-1 (b) patches, 10 days after implantation on cryoinjured rat hearts. Nuclei  
56 are recognized by the blue fluorescence of DAPI. Scale Bars: a and b = 50 $\mu\text{m}$ . Bar graph in c  
57  
58  
59  
60

1  
2  
3 documents the increased number of GFP<sup>pos</sup> rCPCs on IGF-1 functionalized alginate/gelatin/PDO  
4  
5 patches. \* p<0.05 vs alginate/gelatin/PDO.  
6  
7  
8  
9  
10  
11  
12  
13  
14  
15  
16  
17  
18  
19  
20  
21  
22  
23  
24  
25  
26  
27  
28  
29  
30  
31  
32  
33  
34  
35  
36  
37  
38  
39  
40  
41  
42  
43  
44  
45  
46  
47  
48  
49  
50  
51  
52  
53  
54  
55  
56  
57  
58  
59  
60

For Peer Review

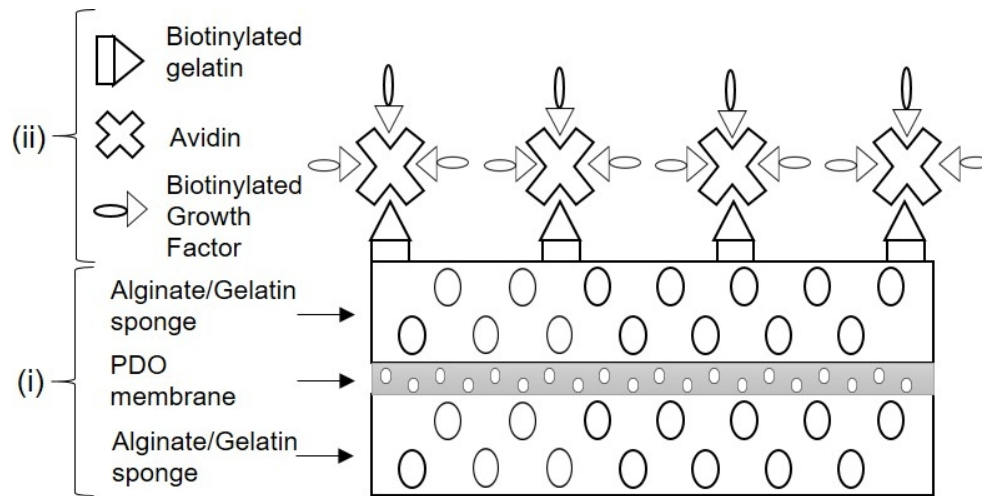


Figure 1. Schematic representation of the alginate/gelatin cardiac patch developed in this work, comprising: (i) reinforcement with PDO membrane, for improved suture resistance; (ii) IGF-1 immobilization, through avidin-biotin binding strategy.

135x67mm (150 x 150 DPI)

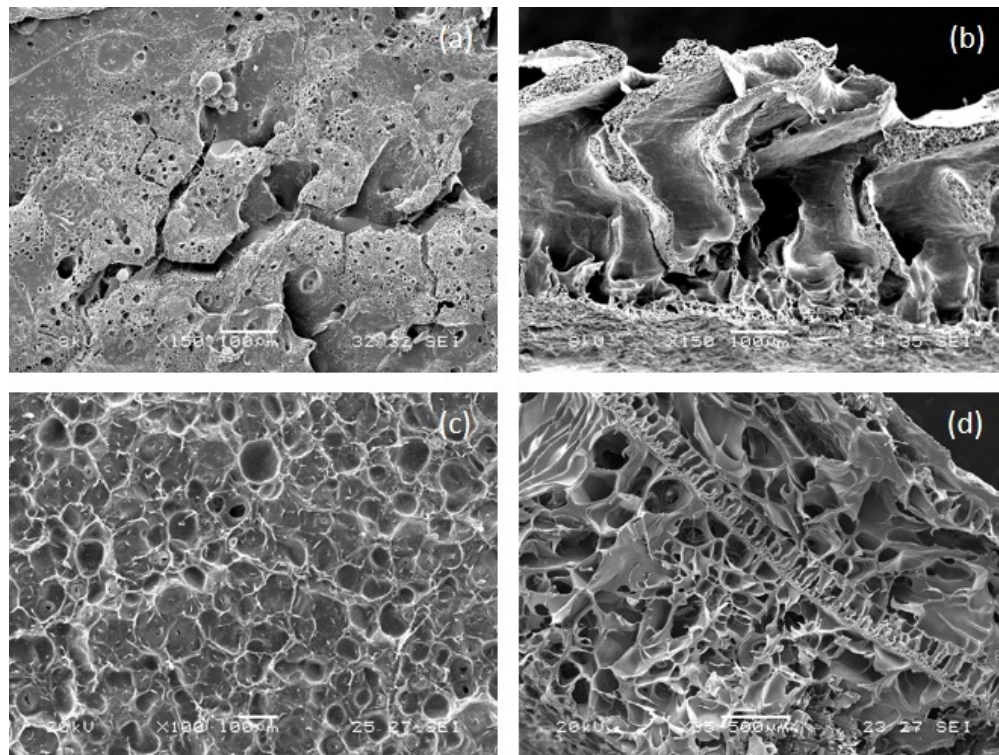


Figure 2. SEM micrographs of PDO membrane, (a) surface and (b) section; PDO reinforced alginate/gelatin scaffolds, (c) surface and (d) section.

111x84mm (150 x 150 DPI)

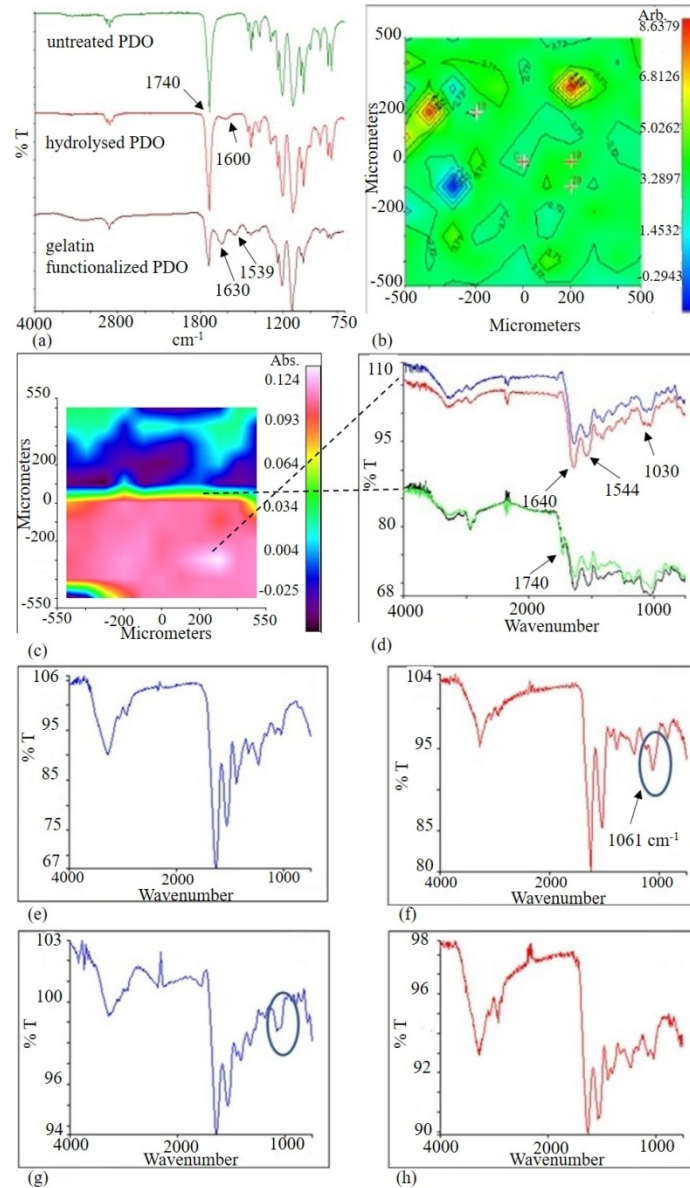


Figure 3. (a) Infrared spectra of untreated PDO, hydrolysed PDO and gelatin functionalized PDO; (b) Chemical map of PDO membrane functionalized with gelatin, in function of the band ratio between the band at 1780-1714  $\text{cm}^{-1}$  (due to PDO) and the band at 1714-1595  $\text{cm}^{-1}$  (due to gelatin); (c) Chemical map of alginate/gelatin sponge reinforced with PDO; (d) Spectra from the chemical map in (c). (e-h) Infrared medium spectra of: (e) biotinylated scaffold; (f) avidin; (g) scaffold treated with avidin and (h) scaffold functionalized with biotinylated growth factor.

167x283mm (150 x 150 DPI)



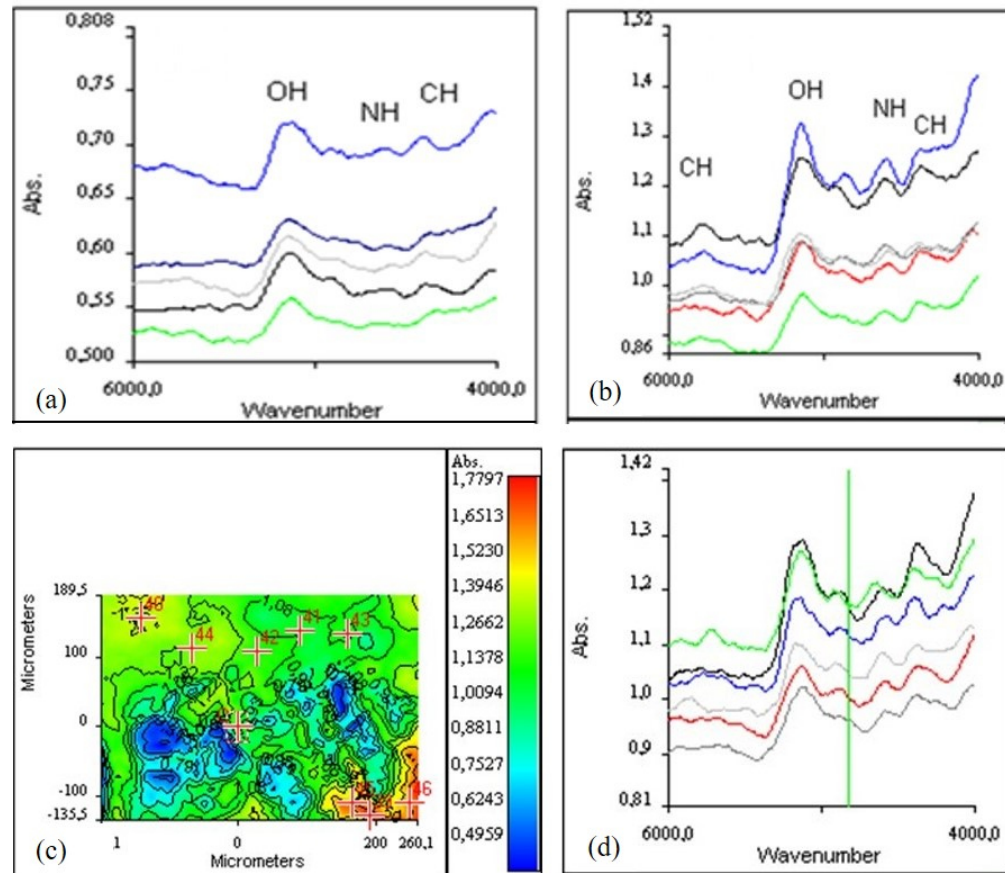


Figure 4. (a) NIR spectra of not functionalized alginate/gelatin/PDO sponge; (b) NIR spectra of alginate/gelatin/PDO sponge, after dipping in biotinylated gelatin; (c) NIR chemical map in function of biotin absorption peak at 4800 cm<sup>-1</sup>; (d) spectra acquired in different areas of the NIR chemical map.

150x132mm (150 x 150 DPI)

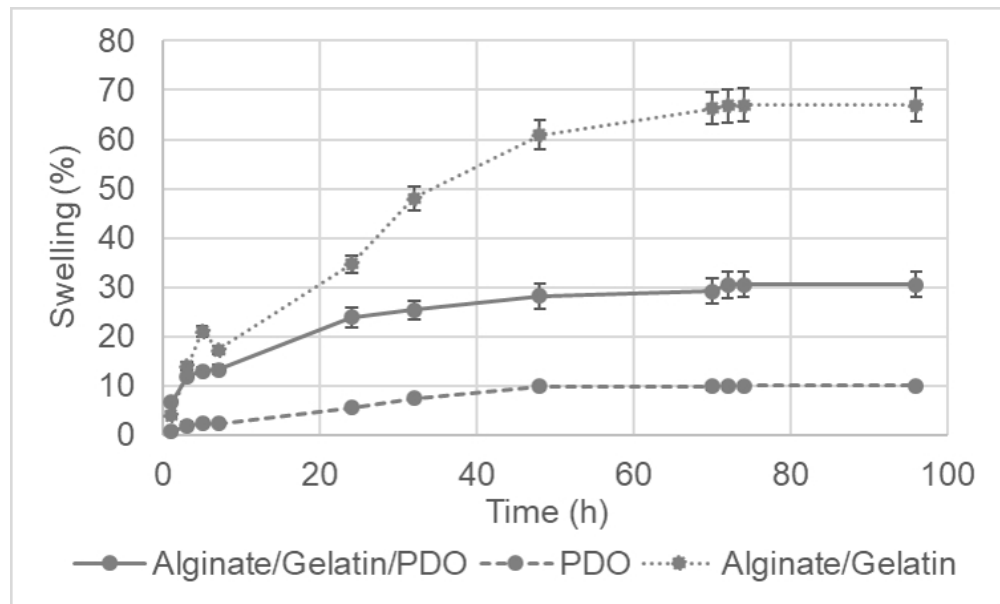
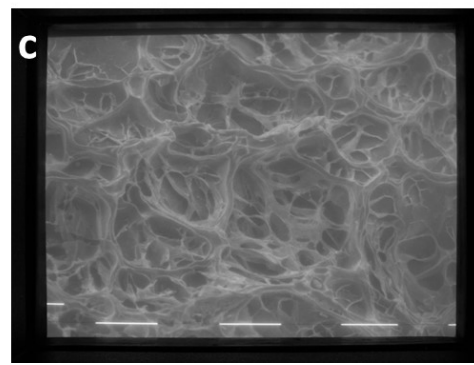
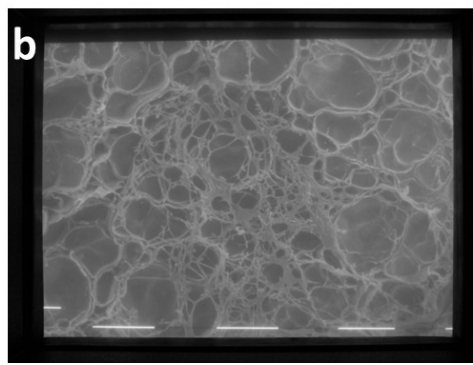
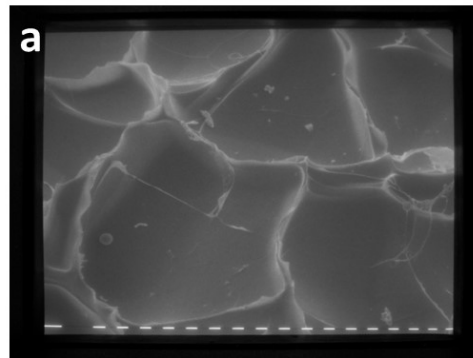


Figure 5. Swelling kinetic for PDO membrane and for alginate/gelatin/PDO scaffolds. Swelling test was performed by exposure to aqueous vapour. Results were compared with those obtained for not reinforced alginate/gelatin scaffolds [8].

127x76mm (150 x 150 DPI)



31 Figure 6. SEM images of rCPCs two weeks after seeding on alginate/gelatin/PDO (a), alginate/gelatin/PDO +  
32 IGF-1 0.9  $\mu\text{g}/\text{cm}^2$  (b) and alginate/gelatin/PDO + IGF-1 1.6  $\mu\text{g}/\text{cm}^2$  (c). Scale bars: a=10 $\mu\text{m}$ , b and  
33 c=100 $\mu\text{m}$ .

34 177x134mm (150 x 150 DPI)

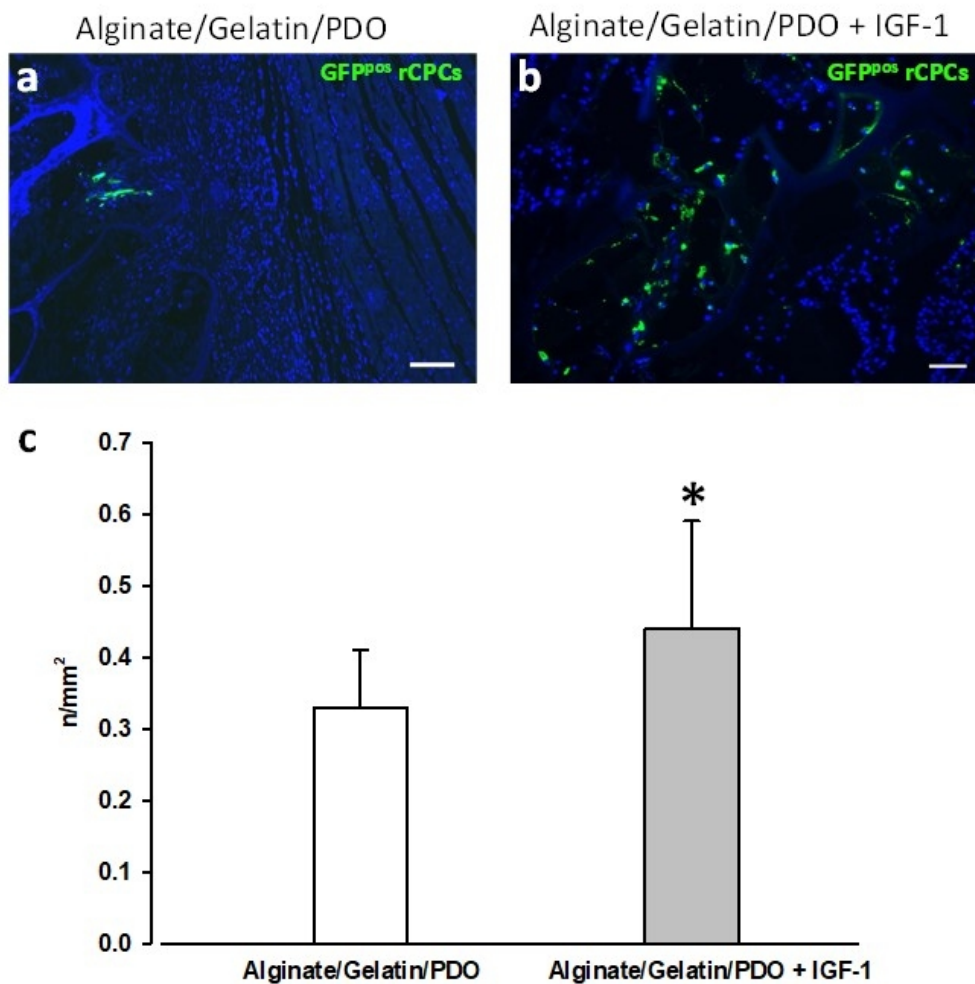


Figure 7. Immunofluorescence detection of GFP<sup>pos</sup> rCPCs (Green) on alginate/gelatin/PDO (a) and alginate/gelatin/PDO + IGF-1 (b) patches, 10 days after implantation on cryoinjured rat hearts. Nuclei are recognized by the blue fluorescence of DAPI. Scale Bars: a and b = 50µm. Bar graph in c documents the increased number of GFP<sup>pos</sup> rCPCs on IGF-1 functionalized alginate/gelatin/PDO patches. \* p<0.05 vs alginate/gelatin/PDO.

111x116mm (150 x 150 DPI)